Anti-Cancer Drug Delivery Modeling in Nanomedicine with Combinatorial Image Analysis and Non-Linear Regression

Sanjay Goswami[1*], Kshama D. Dhobale[2], Ravindra D. Wavhale[2], Barnali Goswami[3], Shashwat S. Banerjee[2*]

[1]Center for Disaster Preparedness and Management, Jadavpur University, Kolkata, India.

[2]Maharashtra Institute of Medical Education and Research, Talegaon Dabhade, Pune-410507, India.

[3]School of Computer Science, Dr. Vishwanath Karad MIT World Peace University, Pune-411038, India.

*Correspondence should be addressed to S.G (sanjaygoswamee@gmail.com), S.S.B (shashwatbanerjee@mitmimer.com)

ABSTRACT

Purpose: The field of cancer *nanomedicine* has made significant progress, but its clinical translation is impeded by many challenges, such as the difficulty in analysing intracellular anticancer drug release by the nanocarriers due to the lack of suitable tools. Here, we propose the development of a combinatorial imaging and analysis technique to evaluate anticancer drug such as *doxorubicin HCl (DOX)* released by a nanocarrier inside the HCT116 colon cancer cells and its subsequent intracellular accumulation.

Procedure: Fluorescent cell images were captured and subjected to combined image analysis and machine learning based procedures to assess and quantify the delivery and retention rate of DOX inside the cancer cells by multifunctional CNT-DOX-Fe_3O_4nanocarrier.

Results: We show that DOX in HCT116 cells was higher for multifunctional CNT-DOX-

Fe_3O_4nanocarrierthan free DOX, indicating efficient and steady release of DOX as well as superior retentive property of the nanocarrier. Initially (1 h and 4 h) the luminance intensity of DOX in the cell cytoplasm delivered by CNT-DOX-Fe_3O_4nanocarrier was ~0.34 times and ~0.42 times lesser than that of free DOX delivered normally. However, at 24 h and 48 h post treatment the luminance intensity of DOX for CNT-DOX-Fe_3O_4nanocarrier was *~1.98 times and 1.92 times higher* than that of free DOX. Furthermore, the luminance intensity of DOX for CNT-DOX-Fe_3O_4in the whole cell was ~1.35 times and ~1.62 times higher than that of free DOX at 24h and 48 h, respectively.

Conclusions: The high-throughput nature of our image analysis workflow allowed us to automate the process of DOX retention analysis, and enabled us to devise machine learning-based modeling to predict the percentage of anticancer drug *retention in cells*. The development of models to automatically quantify and predict intracellular drug release in cancer cells could benefit personalized treatments by optimizing the design of nanocarriers.

Keywords: *Bio-Image Analysis, Computer Vision, Machine Learning, Predictive Modeling, Nanocarriers, Cancer*

1. INTRODUCTION

Nanotechnology has immensely contributed in the evolution of precision medicine as it offers many benefits and opens new opportunities to address the complexity of cancer [1-3]. Moreover, nanotechnology has opened up new opportunities in designing efficient drug-carrier system for cancer therapy [4-6]. Several studies have been carried out to understand the impact of different nanocarrier designs in intracellular delivery of anticancer drugs [7, 8]. Morphologic characteristic of nanocarriers such as size influence the cellular uptake efficiency [9].Hence, it is

imperative to quantitatively know the intracellular anticancer drug released to design an optimum nanocarrier. However, due to the lack of suitable tools to analyze their output, rational designing of nanocarrier platform is extremely difficult [2]. Due to this difficulty, there have been limited studies that probe the anticancer drug delivery and intracellular accumulation of nanocarriers with cancer cells [10]. Integration of artificial intelligence (AI) approaches, using pattern analysis and classification algorithms, can aid in overcoming this gap. Application of AI can help optimize design of nanocarriers by predicting interactions with the targeted cancer cells, in addition to, drug release kinetics, thus affecting therapeutic efficacy [2].AI is a branch of computer science that executes tasks that need "human intelligence." Machine learning (ML), an area of AI, is an approach that trains model using large datasets of previous examples. It is applied in order to find patterns and classify data or find an optimal solution to a given problem. Machine learning and AI in general have been used in different fields of medicine including medical imaging and analysis of gene expression patterns.

Here, we propose the development of a combinatorial imaging and analysis technique to evaluate anticancer drug such as *doxorubicin HCl* (DOX) delivery by nanocarriers inside the HCT116 colon cancer cells and intracellular accumulation. This is achieved by using luminance microscopy to image DOX distribution within HCT116 cells followed by machine learning-based segmentation and image analysis. Our method can automatically and efficiently identify DOX's presence in HCT116 cells. This allows us to measure the amount of DOX delivered by nanocarrier to the cancer cells. For this study, we have used a multifunctional nanocarrier designed by chemically conjugating Fe_3O_4 *NPs*, to Carbon Nano Tubes (CNT) through reactive spacer Glutathione (GSH) and loading of anticancer drug DOX in the cavity of CNT[11]. CNT platform was utilized as a cargo for the cancer therapy because it can

internalize into mammalian cells easily [12]. Furthermore, it offers the benefit of easy surface modification, allowing incorporation of multiple components by conjugation chemistry [13]. Importantly, functionalized CNTs are compatible with biological fluids and leads to their rapid excretion, thus showing low toxicity [12, 14].The advantage of anchoring Fe_3O_4 *NPs* is to impart magnetic property to the nanocarrier. DOX was used as a model anticancer drug in the present study because it is widely utilized in the treatment of a broad spectrum of tumors and in addition possess fluorescence capability. The study will help understand the ability of nanocarriers in interacting with cancer cells, and intracellular drug release kinetics, thus helping in design optimum nanocarriers for effective anticancer drug delivery.

2. METHODOLOGY

The objective of this exercise is to identify a hidden trend in drug delivery and retention through traditional methods as well by nanocarriers, and identify effectiveness of nanocarriers in this context. In the present study, as a model anticancer drug, we have used *doxorubicin HCl* (DOX). DOX is a widely utilized anticancer drug used in the treatment of a broad spectrum of tumors. Furthermore, it also possesses fluorescence capability. Fluorescence of HCT 116 cells when exposed to free DOX and CNT-DOX-Fe_3O_4nanocarrierwill have a direct correlation with the entry and *retention* of DOX inside the cells. Hence, by machine learning-based image analysis we tried to measure DOX accumulation and retention. *Pixel luminance* is considered to be a direct measure of fluorescence in digital images. Hence, luminance of images is calculated henceforth for the purpose. Luminance also directly correlates with the amount of drug accumulation inside the cell.

A. Materials

Multi-walled Carbon Nano Tubes (CNTs) of purity >99% and having outer diameter of 10-15 nm; length 1-5 μm were procured from Ad-Nano Technologies, India. Ferrous chloride hexahydrate, ferric chloride tetrahydrate, *N*-(3-Dimethylaminopropyl)-*N*′-ethylcarbodiimide (EDC.HCl) and glutathione (GSH), McCoy's 5A, fetal bovine serum (FBS), Penicillin and streptomycin were purchased from Sigma-Aldrich, USA. Doxorubicin hydrochloride (DOX) was received from Naprod Life Sciences, India as a gift. HCT116 cells were purchased from the National Centre for Cell Science, India. Ultrapure water (MilliQ) from a Merck Millipore system, Germany, was used throughout. All other chemicals utilized were of analytical grade.

B. Synthesis of CNT-DOX-Fe_3O_4nanocarrier

The Synthesis scheme of DOX loaded CNT-DOX-Fe_3O_4nanocarrieris presented in **Figure 1**. CNT-DOX-Fe_3O_4NPs were prepared using a procedure previously reported by us [11]. In brief, 5 mg of Fe_3O_4 NPs prepared by co-precipitation of ferric and ferrous ions (2:1) were mixed with 4 mg of GSH in 200 μL solution of ultra-pure water and 50 μL of methanol to form Fe_3O_4-GSH. Then, 20 mg of Fe_3O_4-GSH was agitated with 20 mg of oxidized CNT loaded with DOX for 30 min in 5 mL of phosphate buffer (pH 7.4) also containing 5 mg of EDC. The conjugated CNT-DOX-Fe_3O_4 NPs were separated magnetically and washed thoroughly using phosphate buffer and then dried at 40 °C.

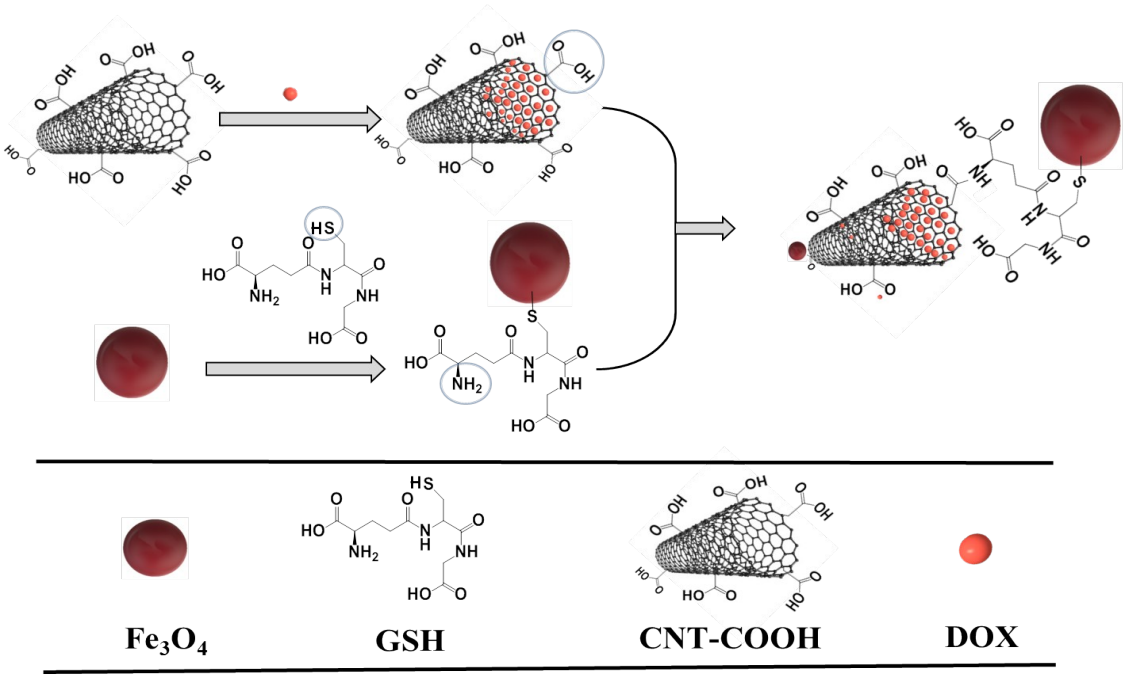

Fig. 1 Synthesis scheme of DOX loaded CNT-DOX-Fe_3O_4nanocarrier.

C. Cell Culture

HCT116 cells obtained from NCCS were cultured in McCoy's cell culture medium supplemented with 10% fetal bovine serum and 100 unit/mL penicillin, 100 mg/mL streptomycin and maintained in CO_2 incubator at 37 °C and 5% CO_2.

D. Time Dependent Cellular Entry Studies using Fluorescence Microscopy

5000 HCT116 cells were seeded in each well of 96 well plates. After 24 h, cells were treated in a time dependent manner (1 h, 4 h, 24 h and 48 h) with free DOX and CNT-DOX-Fe_3O_4nanocarrier and the concentration of DOX was 0.377 µg/mL (IC50). The free DOX and the nanocarrier loaded with DOX (60 µg/mg) were added according to the IC50 value of DOX. The cells were washed with phosphate buffered saline (PBS) after removing the media at consecutive time points and processed for fluorescence microscopy. Cells were fixed with 4.0% (w/v) *paraformaldehyde* for 15 min at room temperature and then maintained in PBS after washing with PBS. Cells were

examined under a fluorescence microscope (Carl Zeiss, Axio Observer A3, USA) after staining with 4,6-diamidino-2-phenylindole (DAPI) (Sigma).

E. Artificial Intelligence Workflow Adopted

Figure2 describes the overall AI workflow adopted to devise the *Luminance Prediction Model* from cell images. At first, *cell images* were obtained using a fluorescence Microscope. Then they are passed over to *Computer Vision Module* for analysis and extraction of *Average Luminance Values* as image features. Then features are sent over to *Machine Learning Module* that learns the model from cell luminance data to come up with a *Luminance Prediction Model* that can be used for generalization of future accumulation trends.

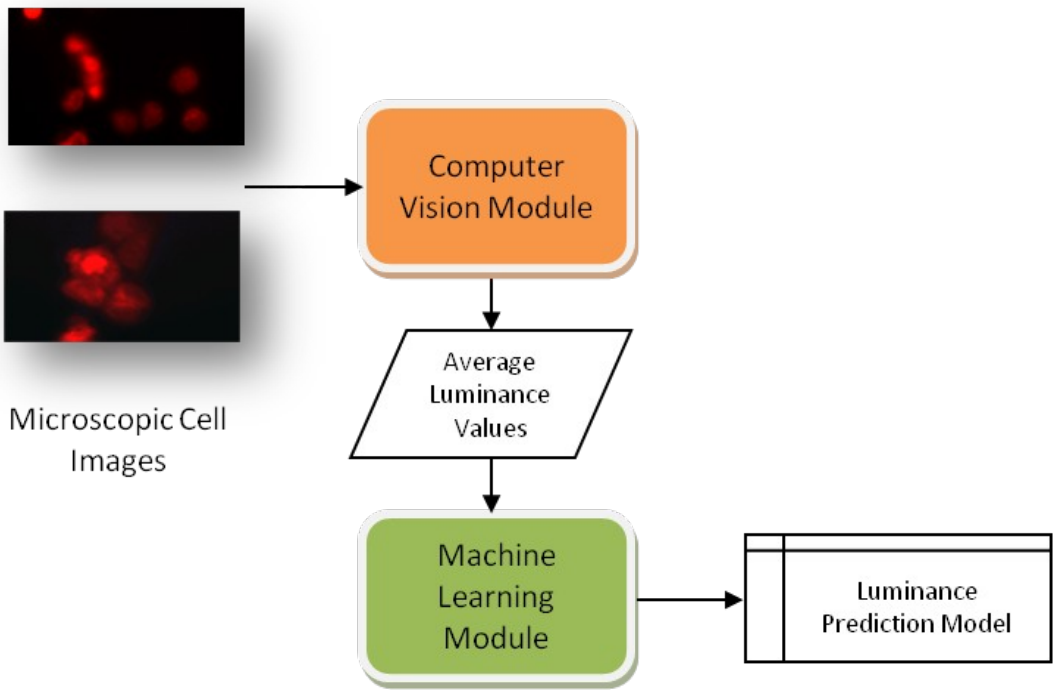

Fig. 2 Artificial Intelligence workflow adopted for the process.

F. Full Cell Imaging Using Fluorescence Microscopy

The cellular uptake and retention of DOX was studied over time by luminance cell imaging. Luminance of cells is a direct measure of drug concentration in the cell. HCT116 cells incubated with DOX, CNT-DOX-Fe_3O_4were examined under fluorescence microscope at definite time intervals. Figures 3aand3b show the cell fluorescence images of HCT116 cells.

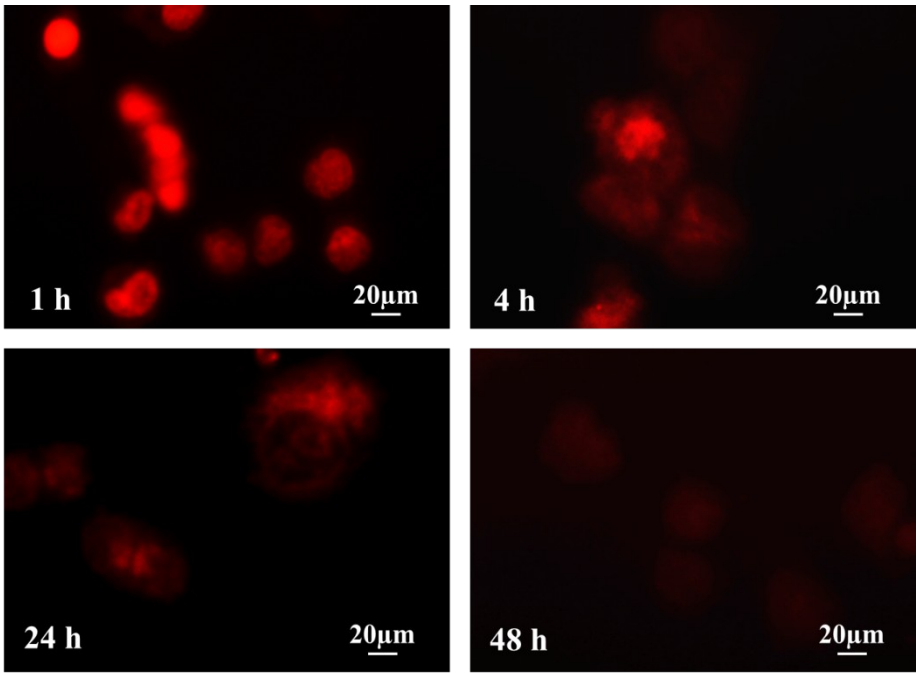

Fig. 3aHCT116 Cell images treated with FREE DOX at different times.

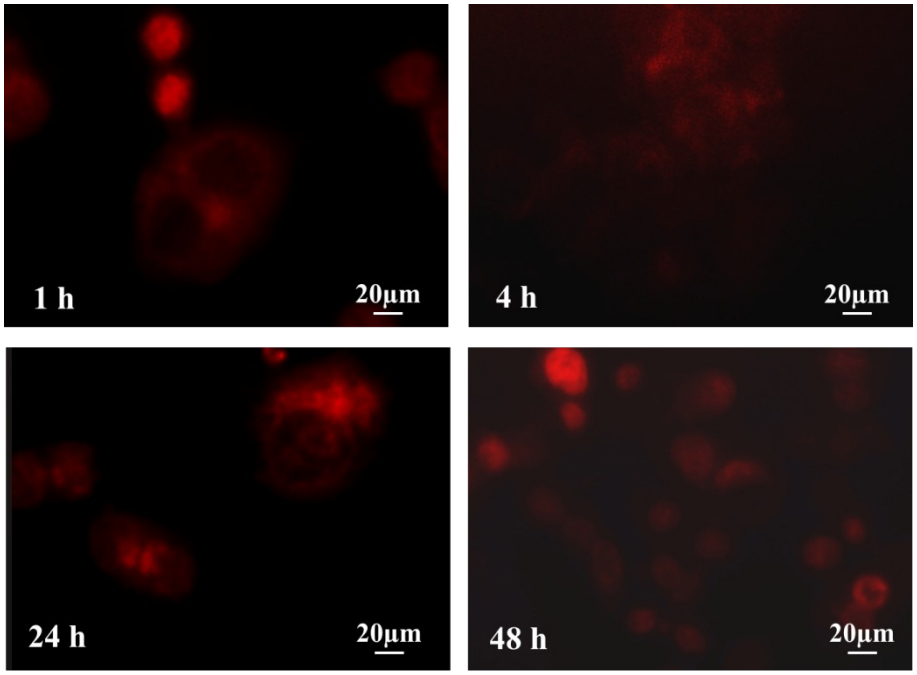

Fig. 3bHCT116 Cell images treated with CNT-DOX-Fe_3O_4 at different times.

G. Extraction of Cytoplasm Images by Image Arithmetic between Full Cell and Nucleus Images

From the lab experiments, full cell composite luminance images were obtained. Separately, nucleus luminance images were obtained after staining them with DAPI. By performing pixel level subtraction between RGB colour images of Full Cell Composite and Nucleus Luminance Images, the Cytoplasm images were extracted. The arithmetic is straight forward as shown in **Figure 4a**.

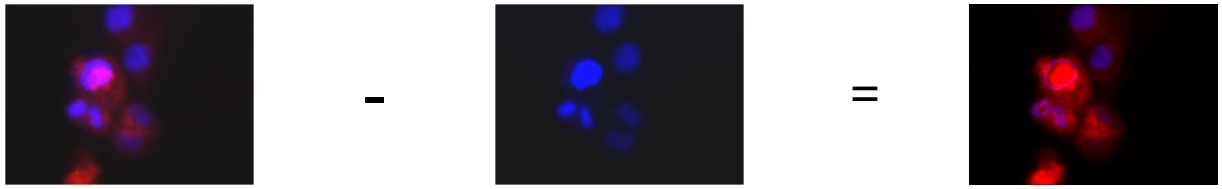

Fig. 4a Image arithmetic between Full Cell Composite &Nucleus images to extract cytoplasm images.

These Cytoplasm images were further studied for DOX retention rates in the cytoplasm.

H. Computer Vision Workflow for Feature Extraction from Microscopic Images

Figure 4bshows the *Computer Vision* workflow adopted to extract features from the microscopic images. Since, *Pixel Luminance* is a measure of *fluorescence* in the cells. Hence, the luminance is calculated.

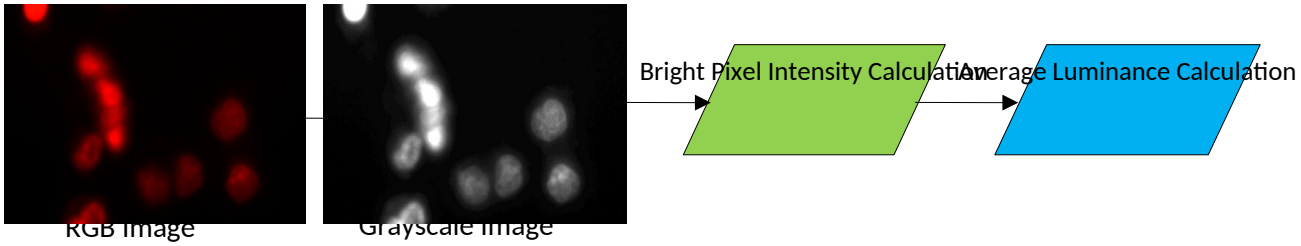

Fig. 4b Computer Vision workflow for average luminance calculation.

Total intensity of bright pixels present in the grayscale image is calculated by measuring the

intensities of the individual bright pixels and taking their sum. That is

$$TotalIntensity(I) = \sum_{i=1}^{n} (PixelIntensity)i \qquad (1)$$

$$Averageluminance = \frac{TotalIntensity(I)}{TotalBrightPixels(n)} \qquad (2a)$$

$$Norm.Avg.luminance = \frac{Avg.luminance}{max\ (Avg.luminance)} \qquad (2b)$$

I. Statistical Visualization of Extracted Data to Identify Model Type

1) Free DOX treated cell and cytoplasm scatter plots

The set of *Time – Luminance* values for free DOX treated cell and cytoplasm images are given in *Tables 1a & 1b*.

Where 'x' represents Time (hours) the HCT116 cells were exposed to free DOX, and 'y' represents Normalized Average Luminance, which is obtained by dividing the entire value set with the maximum value in the group, to slash the set to [0, 1], in order to have a uniform scale across all measurements.

Scatter diagrams plotted for data from *Tables 1a & 1b*, between *Time (h)* and *Normalized Avg. Luminance*, are shown in *Figures 5*, indicates a *non-linearity* in the data.

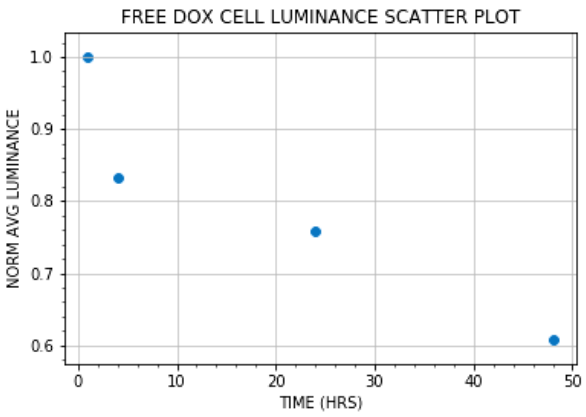

(a)

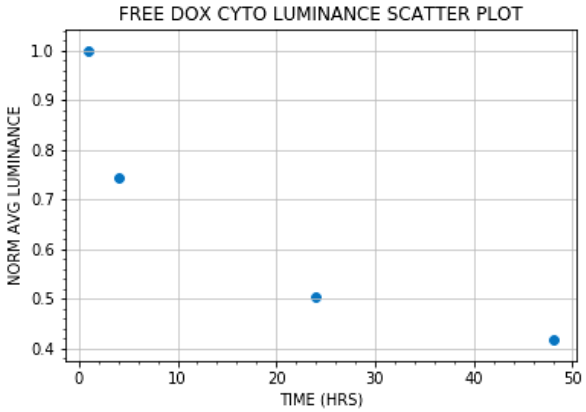

(b)

Fig. 5*Time-Luminance* scatter plots for free DOX treated HCT116 cell images. (a) Full Cell and (b) Cytoplasm.

2) CNT-DOX-Fe_3O_4treated cell and cytoplasm scatter Plots

The set of *Time – Luminance* values for CNT-DOX-Fe_3O_4treated cell and cytoplasm images are given in Tables 2a & 2b:

Scatter diagrams plotted for data from *Tables 2a & 2b*, between *Time (h)* and *Normalized Average Luminance*, are shown in *Figures 6*, which also indicate non-*linearity* in the data.

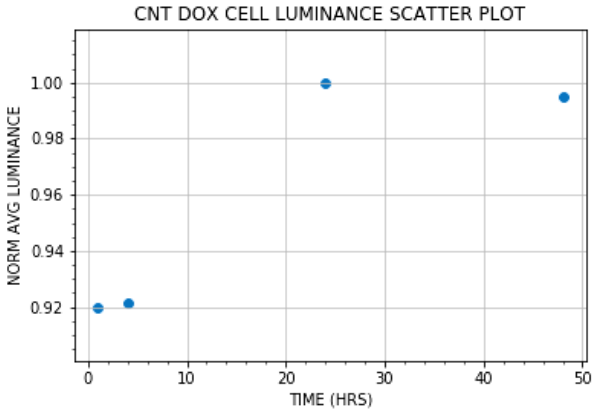

(a)

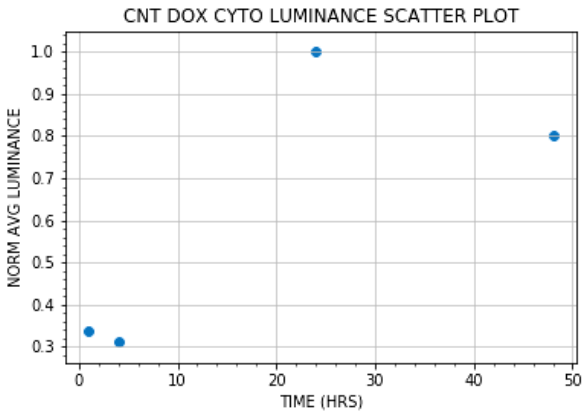

(b)

Fig. 6*Time-Luminance* scatter plots for CNT-DOX-Fe_3O_4 treated (a) Full cell and (b) Cytoplasm.

J. *Statistical Machine Learning for Model Identification*

Looking at the scatter plots, *Least Squares Regression Parabola* seems to be a good *Non-linear Regression* tool that generalizes the data obtained from lab experiments.

The *Least Squares Parabola* equation that fits a given set of data can be written as [13]

$$y = a + bx + c\,x^2 \qquad (3)$$

Where x is the independent variable, y is dependent variable, and a, b *and* c are regression coefficients. Our objective is to estimate the values of a, b *and* c so that a *non-linear parabolic curve* can be obtained that approximates the given data distribution.

The regression coefficients a, b *and* c can be obtained from solving the following *normal equations*

$$\sum y = na + b\sum x + c\sum x^2 \qquad (4)$$

$$\sum xy = a\sum x + b\sum x^2 + c\sum x^3 \qquad (5)$$

$$\sum x^2 y = a\sum x^2 + b\sum x^3 + c\sum x^4 \qquad (6)$$

The eqn. (4) is obtained by taking summation of both sides of eqn. (3). Eqn. (5) is obtained by multiplying eqn. (3) by x on both sides and then taking summation on both sides. Taking the summation of eqn.(3) after multiplying with x^2, yields eqn. (6).

Now with a given set of *(x, y)* pair values, we can calculate all the summations used in the *normal equations* (4) – (6). Solving these equations with summations properly placed, we can get the values of *a, b and c*. Substituting them in the eqn. (3) yields the *Least Squares Regression Parabola* equation.

K. Least Squares Regression Curves Generation

a) *For free DOX treated Cell images*

By going through the procedure discussed in section 2.*E,* the *Least Squares Regression Parabola* equation for *free DOX treated cell images, as* obtained by the model on learning from data given in *Table 1a* is:

$$y = 0.974680 - 0.012915\,x + 0.000114\,x^2 \quad (7)$$

The Residual Least Square Error is = 0.0009444

The *Regression Parabola Curve* to generalize the accumulation kinetics is shown in the *Figure 7.*

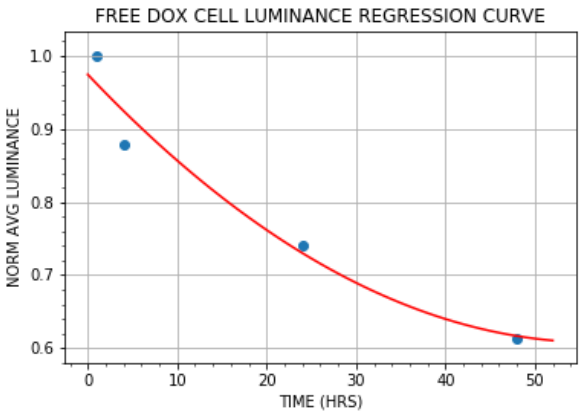

Fig. 7 Time-Luminance Regression Parabola for free DOX treated Full Cell images.

b) *For free DOX treated cytoplasm images*

The *Least Squares Regression Parabola* equation for *free DOX treated cytoplasm images* as learned from data given in *Table 1b* is:

$$y = 0.948587 - 0.027997\,x + 0.000356\,x^2 \qquad (8)$$

The Residual Least Square Error is = 0.0040616

The corresponding *Regression Parabola Curve* to generalize the reaction kinetics as per equation identified in *eqn.8* is shown in the *Figure 8.*

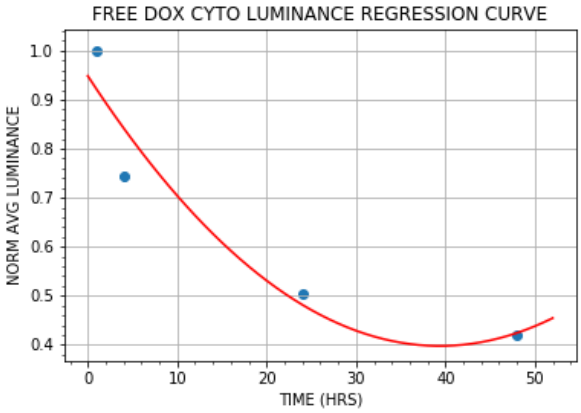

Fig. 8*Time-Luminance* Regression Parabola for free DOX treated Cytoplasm images.

c) CNT-DOX-Fe_3O_4treated cell images

The *Least Square Regression Parabola* Equation learned from the data in *Table 2a* is

$$y = 0.907974 + 0.005695\,x + -0.00008\,x^2 \qquad (9)$$

The Residual Least Square Error is = 2.6063603e-05. The corresponding curve is shown in Figure 9.

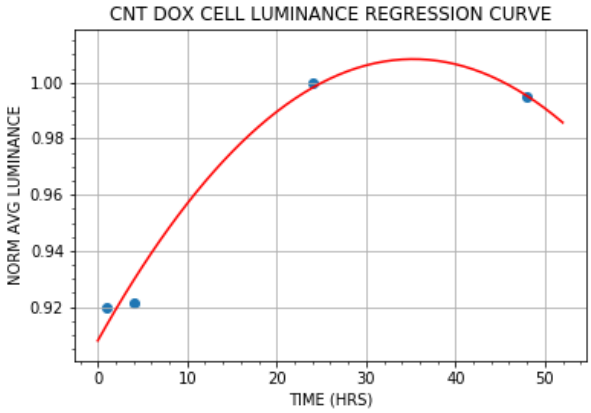

Fig. 9*Time-Luminance* Regression Parabola for CNT-DOX-Fe_3O_4 treated full cell images.

d) CNT-DOX-Fe_3O_4treated Cytoplasm images

The *Least Squares Regression Parabola* Equation obtained from the data given in *Table 2b* is

$$y = 0.211136 + 0.051466\,x + -0.000813\,x^2 \qquad (10)$$

The Residual Least Square Error is = 0.0037100. The corresponding curve is shown in Figure 10.

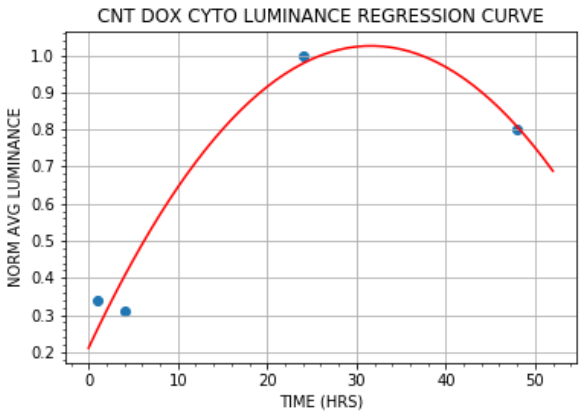

Fig. 10*Time-Luminance* Regression Parabola for *CNT-DOX-Fe_3O_4 treated* Cytoplasm images.

3. RESULTS AND DISCUSSIONS

The Regression Polynomials obtained in the equations (7) – (10), have *Least Square Residual Errors* as *0.0009444, 0.0040616, 2.6063603e-05 & 0.0037100,* respectively. Given the number of data points and the corresponding residual errors, it can be seen that the errors are very less. This implies that the corresponding curves are nearly perfect fit. These polynomials can be used to model anticancer drug treatment outcomes in the future, given the same reaction parameters and conditions.

Studying the Cell Luminance normalized values, it is found that initially in the *1 h* the luminance intensity of DOX delivered in the cell through CNT-DOX-Fe_3O_4nanocarrier was ~0.34 times lesser than that of free DOX delivered normally. At*4 h* post treatment, the luminance intensity of DOX delivered through CNT-DOX-Fe_3O_4nanocarrier was ~0.42 times lesser than that of free DOX. However, the luminance intensity of DOX delivered by CNT-DOX-Fe_3O_4 increased and it was *~1.98 times and 1.92 times higher* in the *24h* and*48 h* respectively, than that of free DOX. Furthermore, the luminance intensity of DOX delivered through CNT-DOX-Fe_3O_4 in the whole

cell was ~1.35 times and ~1.62 times higher than that of free DOX at *24h* and *48 h*, respectively.

From the Regression Parabola plots also, it is observed that when free DOX is administered then the drug enters the HCT116 cell fast, but also effluxes fast. This property is evident from both the plots, Figure 7 and 8, depicting free DOX accumulation and retention rate in both full cell and cell cytoplasm.

However, when the DOX is administered using CNT-DOX-Fe_3O_4nanocarrier, the drug initially enters the HCT116 cells slowly, but gradually increases and is then retained in the cell for a long time. This phenomenon is evident from the plots in Figures 9 and 10. From these figures it can be seen that DOX concentration in the cells increases gradually till 4h. However, the concentration increases sharply till the 24h and remains with a considerable concentration till 48 h.

4. CONCLUSION

The objective of this computational exercise was to model a combinatorial imaging and analysis technique to evaluate delivery of *DOX* by nanocarriers inside the cancer cells and its subsequent intracellular accumulation. A *Polynomial Regression Model*, created by Statistical Machine Learning, did this satisfactorily even though with cell images available at only four time points. The predicted intermediate values of the model reveal that DOX delivered by the multifunctional CNT-DOX-Fe_3O_4nanocarrier in HCT116 colon cancer cells is higher which is in correlation with human cognizable insights. Furthermore, the model confirms that DOX delivery with CNT-DOX-Fe_3O_4nanocarrieris *far more effective* than free delivery. This model appears to be a good regression tool that can be used for future research involving reaction kinetics modeling with very small data set.

ACKNOWLEDGMENT

The authors acknowledge the financial support of Department of Biotechnology, and Department of Science and Technology, Government of India.

CONFLICT OF INTEREST

The authors declare that they have no conflict of interest.

REFERENCES

1. Ferrari M (2005) Cancer nanotechnology: opportunities and challenges Nat Rev Cancer 5:161-171.
2. Adir O, Poley M, Chen G, Froim S, Krinsky N, Shklover J, Shainsky-Roitman J, Lammers T, Schroeder A(2020) Integrating Artificial Intelligence and Nanotechnology for Precision Cancer Medicine Adv Mater 32:1901989-1902004.
3. KhandareJJ, Jalota-Badhwar A, TanejaN, Mascarenhas RR, Vadodaria K, Zope KR, Banerjee SS(2013) Fabrication of pH-Tunable Calcium Phosphate Nanocapsules via Dendrimer-Templated Assembly for Intracellular Lysosomal Release of Drugs Part Part Syst Charact 30:494-500.
4. Peer D, Karp JM, Hong S, Farokhzad OC, Margalit R, Langer R (2007)Nanocarriers as an emerging platform for cancer therapy Nat. Nanotechnol 2:751-60, 2007.
5. Banerjee SS, Jalota-Badhwar A, Satavalekar SD, Bhansali SG, Aher ND, Mascarenhas RR, Paul D, Sharma S, Khandare JJ (2012) Transferrin-mediated rapid targeting, isolation, and detection of circulating tumor cells by multifunctional magneto-dendritic nanosystem Adv Healthcare Mater 2: 800-805.

6. Banerjee SS, Jalota-Badhwar A, Zope KR, Todkar KJ, Mascarenhas RR, Chate GP, Khutale GV, Bharde A, Calderon M, Khandare JJ(2015) Self-propelled carbon nanotube based microrockets for rapid capture and isolation of circulating tumor cells Nanoscale 7:8684-8688.
7. Jain RK, Stylianopoulos T (2010) Delivering nanomedicine to solid tumors, Nat Rev Clin Oncol 7:653-664.
8. Banerjee SS, Jalota-Badhwar A, WateP, AsaiS, ZopeKR, MascarenhasR, BhatiaD, KhandareJ (2014) Structure effect of carbon nanovectors in regulation of cellular responses Biomater Sci 2:57-66.
9. Dimitri A,TalamoM (2018) The use of data mining and machine learning in nanomedicine: A surveyFrontiers in Nanoscience and Nanotechnology 4: 1-7.
10. Kingstona BR, Syeda AM, Ngaia J, Sindhwania S, Chana WCW (2019) Assessing micrometastases as a target for nanocarriers using 3D microscopy and machine learning, Proc Nat AcadSci 116:14937-14946.
11. Andhari SS, Wavhale RD, Dhobale KD, Tawade BV, Chate GP, Patil YN, Khandare JJ, Banerjee SS (2020) Self-propelling targeted magneto-nanobots for deep tumor penetration and pH-responsive intracellular drug delivery Sci Rep 10:4703-4718.
12. Yan H, Xue Z, Xie J, Dong Y, Ma Z, Sun X, KebebeBorga D, Liu Z, Li J (2019) Toxicity of Carbon Nanotubes as Anti-Tumor Drug Carriers, Int J Nanomedicine14:10179-10194.
13. Sun YP, Fu K, Lin Y, Huang W (2002) Functionalized Carbon Nanotubes: Properties and Applications Acc Chem Res 35:1096-104.
14. Spiegel MR, Schiller J, Srinivasan RA(2013) Schaum's Outlines on Probability &Statistics,4th ed., McGraw-Hill, New York, p 265-313.

Tables

Table 1a: Time – Luminance data for free DOX treated HCT116 Cell images

Time (x) (h)	1	4	24	48
Norm. Avg. Lum. (y)	1.0	0.878012	0.741396	0.614171

Table 1b: Time – Luminance data for free DOX treated HCT116 cell Cytoplasm images

Time (x) (h)	1	4	24	48
Norm. Avg. Lum. (y)	1.0	0.745175	0.504721	0.418948

Table 2a: *Time – Luminance* data for CNT-DOX-Fe_3O_4 treated HCT116 Cell images

Time (x) (Hr)	1	4	24	48
Norm. Avg. Fluo. (y)	0.919921	0.921683	1.0	0.994856

Table 2b: *Time – Luminance* data for CNT-DOX-Fe_3O_4 treated HCT116 Cytoplasm images

Time (x) (Hr)	1	4	24	48
Norm. Avg. Fluo. (y)	0.337344	0.311171	1.0	0.802517

Brief Biographies

Sanjay Goswami has a B.Sc from C. S. J. M. University, Kanpur (1998), MCA from IGNOU, India (2004) & Ph.D. from Jadavpur University, Kolkata, (2017). His current research interests are ML & its applications in natural & medical disaster mitigation.

Barnali Goswami has a BSc. from MJP Rohilkhand University, India (2001), MCA from IGNOU, India (2004) & Ph.D. from Jadavpur University, India (2016). Currently she is an Asst. Prof. at MIT WPU, Pune. Her research interests include AI and ML in disaster management

Kshama D Dhobale has a M.Sc. (Biotech.) from Pune University (2011). She was aProject Assistant at the Central Research Lab, MIMER, Pune, India (2018-2020). Her research interests include in-vitro small molecule drug screening & imaging.

Ravindra D. Wavhale has a M.Pharm. from Bombay College of Pharmacy, India (2010) & a PhD from same college (2016). He was a RA at the Central Research Lab, MIMER, Pune, India. His research interests include surface chemistry of nanomaterials for biomedical applications.

. **Shashwat S. Banerjee** has a PhD from ICT Mumbai (2003). He was a PDF at NCK University, Taiwan (2003) &WSU (2008). Currently he is heading Central Research Lab at MIMER, Pune, India, involved in design & synthesis of biomaterials to address various medical needs.